

# Improving Cross-dataset Deepfake Detection with Deep Information Decomposition

Shanmin Yang<sup>1</sup>, Shu Hu<sup>2</sup>, Bin Zhu<sup>3</sup>, Ying Fu<sup>1</sup>, Siwei Lyu<sup>4</sup>, Xi Wu<sup>1,\*</sup>, Xin Wang<sup>5,\*</sup>

<sup>1</sup> Chengdu University of Information Technology

<sup>2</sup> Indiana University–Purdue University Indianapolis

<sup>3</sup> Microsoft Research Asia

<sup>4</sup> University at Buffalo, SUNY

<sup>5</sup> University at Albany, SUNY

xi.wu@cuit.edu.cn, xwang56@albany.edu

## Abstract

Deepfake technology poses a significant threat to security and social trust. Although existing detection methods have demonstrated high performance in identifying forgeries within datasets using the same techniques for training and testing, they suffer from sharp performance degradation when faced with cross-dataset scenarios where unseen deepfake techniques are tested. To address this challenge, we propose a deep information decomposition (DID) framework in this paper. Unlike most existing deepfake detection methods, our framework prioritizes high-level semantic features over visual artifacts. Specifically, it decomposes facial features into deepfake-related and irrelevant information and optimizes the deepfake information for real/fake discrimination to be independent of other factors. Our approach improves the robustness of deepfake detection against various irrelevant information changes and enhances the generalization ability of the framework to detect unseen forgery methods. Extensive experimental comparisons with existing state-of-the-art detection methods validate the effectiveness and superiority of the DID framework on cross-dataset deepfake detection.

## 1 Introduction

The significant progress in deep learning and generative techniques such as Face2Face (Thies et al. 2016), DeepFake (Rossler et al. 2019), GANs (Pumarola et al. 2018; Karras, Laine, and Aila 2019a), etc., has enabled the creation of highly realistic face images. However, the widespread use of these deepfakes has posed a significant threat to security and social trust. Therefore, it is crucial to develop effective methods to detect face forgery.

Numerous efforts have been devoted to deepfake detection in recent years. Most existing works focus on specific visual artifacts resulting from the deepfake creation process, such as discrepancies across blending boundaries of real and fake faces (Li et al. 2020a), differences of head poses (Yang, Li, and Lyu 2019), affine face warping artifacts (Li and Lyu 2019), the eye state (Li, Chang, and Lyu 2018), frequency differences (Frank et al. 2020; Qian et al. 2020; Li et al. 2021), etc. Although these methods have achieved promising performance in intra-dataset scenarios where both the

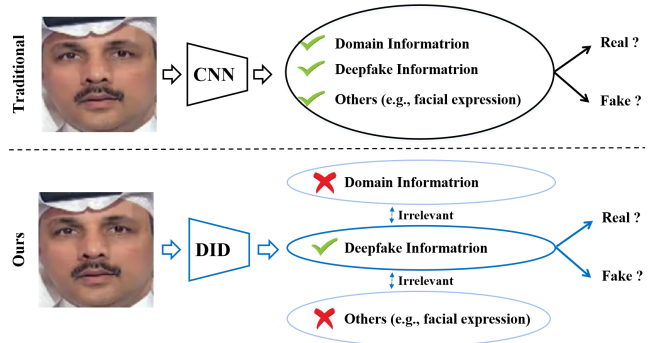


Figure 1: Various information entangled with the deepfake information in traditional methods (**top**) would affect the real/fake classification accuracy, leading to a sharp degradation when changes in these components between the training and test sets are more significant than the difference between real and deepfake information. Our proposed deep information decomposition (DID) method (**bottom**) separates the deepfake information from various information irrelevant to real/fake classification to improve the robustness of deepfake detection.

training and testing face images are created with the same deepfake technique, they are likely to overfit the specific artifacts of the deepfake technique and thus may be ineffective to detect faked faces created with different deepfake techniques. For instance, the detection method proposed in (Qian et al. 2020) achieves an AUC score of 0.98 when both trained and tested on the same FaceForensics++ (FF++) deepfake dataset (Rossler et al. 2019). Its AUC score degrades sharply to 0.65 (Nadimpalli and Rattani 2022; Kim and Kim 2022) when trained on the FF++ dataset and tested on Celeb-DF (Li et al. 2020b).

In studying the cross-dataset performance degradation problem, we observe that deepfake detection is a type of fine-grained image classification. With advances in deep forgery methods, differences between authentic and deep fake images are becoming more and more subtle, even subtler than those between deepfake images synthesized from the same authentic image with different forgery techniques.

\*Corresponding authors.

In addition, features directly extracted with general deep neural networks (e.g., ResNet-50 (He et al. 2016), EfficientNet(Tan and Le 2021), etc.) always include various entangled information, such as forgery technique-related (domain) information and others (e.g., facial expression) as shown in Fig. 1. It makes deepfake detection performance sensitive to any change in any component, especially the most prominent ones.

Motivated by these observations, we propose a Deep Information Decomposition (DID) framework for cross-dataset deepfake detection, as shown in Fig. 2. Unlike existing methods, we focus on high-level semantic features rather than low-level deepfake visual traces. Specifically, we denote face images forged by different deepfake methods as different data domains and formulate cross-dataset deepfake detection as a domain generalization problem. Then, we adaptively decompose the deepfake facial information into deepfake information, forgery technique information (e.g., Face2Face (Thies et al. 2016), DeepFake (Deepfakes)), and others using two attention modules. Only the deepfake information is used for genuine and sham discrimination. Furthermore, we introduce a de-correlation learning module to promote the deepfake information to be independent of irrelevant information, thus improving the detection generalizability to irrelevant variations, including different datasets and different forgery methods. Extensive experiments demonstrate the effectiveness and superiority of our framework. We achieve new state-of-the-art performance on cross-dataset deepfake detection. In summary, our main contributions are:

1. We introduce a new end-to-end Deep Information Decomposition (DID) framework that decomposes deepfake face image information into deepfake information and deepfake-irrelevant information. By formulating cross-dataset deepfake detection as a domain generalization problem, we can improve deepfake detector’s generalization ability.
2. A de-correlation learning module is introduced to encourage the independence of decomposed components without knowing (assuming) their distribution functions or relationships, which can intrinsically improve the robustness of deepfake detection.
3. We conducted extensive experiments that show our framework’s superiority, achieving new state-of-the-art performance on the challenging cross-dataset deepfake detection task.

## 2 Related work

This section provides a brief review of deepfakes, cross-dataset deepfake detection, and information decomposing. For more details about the deepfake techniques and deepfake datasets, please refer to (Nguyen et al. 2022; Karras, Laine, and Aila 2019b). **Deepfakes.** The broad definition of deepfake involves manipulated or synthetic media (e.g., images, sounds, etc.) that seems natural (Zhang 2022; Nguyen et al. 2022). In this paper, we focus on deepfake faces. We classify existing deepfakes into two types, transfer-based and synthesis-based deepfake methods.

A transfer-based deepfake method tries to manipulate target faces by replacing the faces or facial attributes (e.g., expression, mouth, eye, etc.) with reference faces. For example, Face2Face (Thies et al. 2016) reenacts the person in a target video with expressions of another person while preserving the target face identity. FaceSwap (Faceswap) and DeepFakes (Deepfakes) replace the face region of a target video with that in the reference source video. Neural Textures(Thies, Zollhöfer, and Nießner 2019) combines learnable neural textures (from the reference video) with deferred neural rendering to manipulate facial expressions corresponding to the mouth region. The method in (Bao et al. 2018) decouples a face image into identity and attributes and then generates new identity-preserving face images by recombining this identity with attribute features from another face image. Almost all deepfake methods of this type require reference faces and pay attention to blending manipulated and unmanipulated parts to improve deepfake realism.

A synthesis-based method synthesizes non-existing faces or face attributes (e.g., skin color, hair color, etc.) without any reference face. Generative adversarial networks (GAN) and 3D Morphable Models (3DMM) are popularly used in this type of method. For instance, the method in (Geng, Cao, and Tulyakov 2019) proposes a 3DMM-guided way to synthesize arbitrary expressions while preserving the face identity. StyleGAN (Karras, Laine, and Aila 2019b) generates a deepfake dataset with high variety and quality based on a style-based generator. GANprintR (Neves et al. 2020) is a GAN-based method designed to generate entirely realistic deepfake faces.

**Cross-Dataset Deepfake Detection.** With the development of deepfake methods, many deepfake detection methods (Zhao et al. 2021a; Dong et al. 2022b; Shiohara and Yamasaki 2022; Dong et al. 2022a) have also been proposed. They can achieve satisfying performance when testing and training face images are manipulated with the same deepfake method, but suffer from sharp performance degradation when tested on datasets generated with deepfake methods different from those of training datasets. To address this issue, (Zhao et al. 2021b,b) propose dynamic data augmentation methods to generate new data. The method in (Nadimpalli and Rattani 2022) uses a reinforcement learning-based image augmentation model to reduce the cross-dataset (domain) shift. The method in (Yu et al. 2022) aims to capture common forgery features over different forgery datasets. The method in (Luo et al. 2021) relies on high-frequency image noises to reveal forgery traces and improve the cross-modality generalization ability. Focusing on the edge region, the method in (Kim and Kim 2022) detects deepfakes according to color-distribution changes appeared in the face-synthesis process. However, cross-dataset deepfake detection is still a challenging and critical issue.

**Information Decomposing.** Information decomposing aims to decouple entangled information into different semantic components and capture task-related ones. The methods in (Tran, Yin, and Liu 2017; Wang et al. 2019) separate identity-dependent information from pose and age variations, respectively, to reduce the influence of pose/age discrepancy on face recognition. The method in (Wu et al.

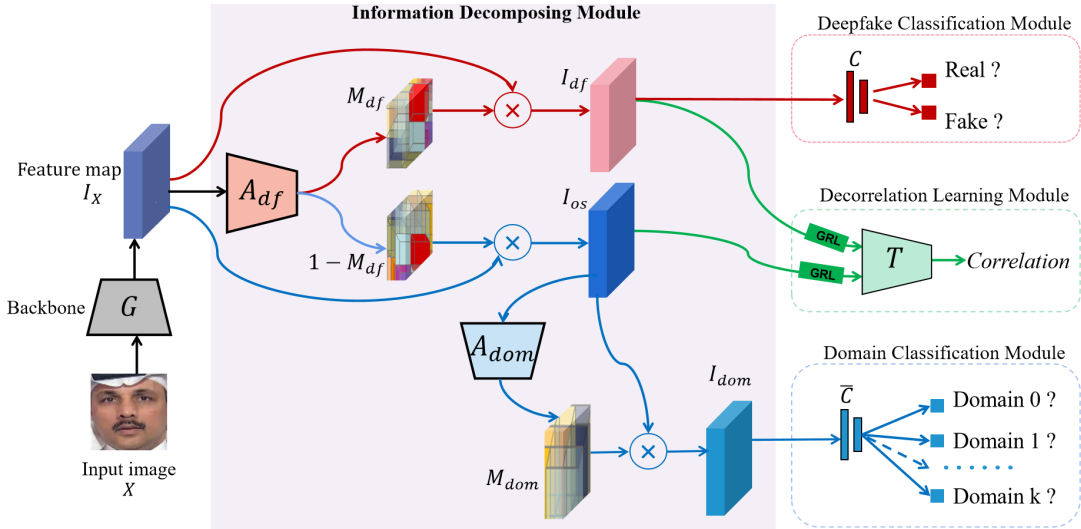


Figure 2: Overview of our Deep Information Decomposition (DID) framework. Feature map  $I_X$  of input face image  $X$  from a backbone network  $G$  is decomposed into deepfake information  $I_{df}$  and non-deepfake information  $I_{os}$  adaptively under the guidance of the deepfake attention network  $A_{df}$  and supervision of the deepfake classification module. The domain attention network  $A_{dom}$  and domain classification module capture the forgery method-related (domain) information  $I_{dom}$  and ensure that  $I_{dom}$  is included in the non-deepfake information but not in the deepfake information. In addition, the decorrelation learning module ensures no overlapping between the deepfake information and non-deepfake information. This module consists of an information estimation network  $T$ , which functions in a max-min manner with the information decomposition module through the gradient reversal layer (GRL).  $C$  and  $\bar{C}$  are the deepfake and domain classifiers, respectively.

2019) disentangles facial representations into identity information and modality information for NIR-VIS heterogeneous face recognition. For deepfake detection, the method in (Hu, Wang, and Li 2021) locates the forgery-related regions via feature disentangling and trains the forgery detector from these regions at different scales. The method in (Liang, Shi, and Deng 2022) separates artifact features from content information to reduce the interference of content information to forgery detection. In this paper, we present an information decomposition framework that achieves disentanglement via complementary attention, unlike those in (Hu, Wang, and Li 2021; Liang, Shi, and Deng 2022) realizing information disentanglement via feature encoding and decoding with three elaborately designed reconstruction loss (i.e., self-reconstruction, cross-reconstruction, and feature reconstruction). In addition, we introduce a deep decorrelation module to further boost the disentangle performance and improve the robustness of deepfake detection to forgery-irrelevant variations.

### 3 Our Method

The pipeline of our proposed method is shown in Fig. 2. Specifically, for an input image  $X$ , we use a CNN-based feature extractor  $G$  parameterized by  $\theta$  to extract its representative features, which can be represented as  $I_X := G(\theta; X)$ . Then we decompose it into three parts: the deepfake-related representation,  $I_{df}$ , which is the main information to be used for detecting deepfakes; the domain-related representation,  $I_{dom}$ , which can be used to track what the associated forgery technique or method that generates it; and the remainder

representation. The information decorrelation module optimizes the decoupled deepfake information  $I_{df}$  to be independent of the other representations and thus enhances the decomposition performance. The robust deepfake classification module is designed to learn a model that can effectively classify deepfakes in the presence of imbalanced datasets and therefore encourages its generalization ability. The domain classification module is designed to identify which domain  $I_{dom}$  belongs to. Before describing these modules, we introduce the commonly used notation.

#### 3.1 Notation

Our method takes images from existing deepfake datasets as input data. Let  $\mathcal{S} = \{(X_i, Y_i, D_i)\}_{i=1}^n$  be a training dataset that contains images  $X_i \in \mathbb{R}^d$  and the corresponding labels  $Y_i \in \{0, 1\}$ , where 0 means real and 1 indicates fake.  $D_i := [D_i^0, D_i^1, \dots, D_i^k]^\top$  represents the domain label of  $X_i$ , where the fake data domain size  $k \geq 1$  and  $D_i^j \in \{0, 1\}, \forall j \in \{0, 1, \dots, k\}$ . In particular,  $D_i^j = 1$  indicates  $X_i$  from the  $j$ -th domain, where  $X_i$  is from the real data domain if  $j = 0$  or from fake data domain  $j$  (i.e., forged by method  $j$ ) if  $j > 0$ . For example, the fake images in the FF++ dataset (Rossler et al. 2019) are generated by four face manipulation methods: Deepfakes (Deepfakes), Face2Face (Thies et al. 2016), FaceSwap (Faceswap), and NeuralTextures (Thies, Zollhöfer, and Nießner 2019). Therefore,  $k = 4$ . In this work, we assume that each  $X_i$  only comes from one domain.

### 3.2 Information Decomposition Module

Inspired by (Yang et al. 2021), the information decomposition module consists of a deepfake attention module and a domain attention module. It decomposes the face information  $I_X$  into deepfake information  $I_{df}$ , forgery technique information  $I_{dom}$ , and others as follows,

$$\begin{aligned} M_{df} &= A_{df}(\psi; I_X), & I_{df} &= M_{df} \otimes I_X, \\ I_{os} &= (1 - M_{df}) \otimes I_X, & M_{dom} &= A_{dom}(\varphi; I_{os}), \\ I_{dom} &= M_{dom} \otimes I_{os}, \end{aligned}$$

where  $A_{df}(\psi; \cdot)$  is the deepfake attention network module parameterized by  $\psi$ . It focuses on the real/fake information with attention map  $M_{df}$  and thus separates  $I_{df}$  from irrelevant information  $I_{os}$ .  $A_{dom}(\varphi; \cdot)$  is the domain attention network aiming at extracting the domain information with attention map  $M_{dom}$ , and thus decouples  $I_{os}$  into domain information  $I_{dom}$  and the rest information.  $\otimes$  represents the Hadamard product.

### 3.3 Decorrelation Learning Module

The disentangled components (deepfake information and non-deepfake information) are expected to be distributed in two distinct parts. To this end, orthogonal constraints are usually employed on these disentangled components (He et al. 2017, 2018; Wang et al. 2019). However, linear dependence/independence can hardly characterize the complex relationship between deepfake information and non-deepfake information in a high-dimensional and nonlinear space. In contrast, mutual information (Kinney and Atwal 2014) can capture arbitrary dependencies between any two variables.

With this motivation, we apply mutual information to evaluate dependencies between deepfake information  $I_{df}$  and non-deepfake information  $I_{os}$ , formulated as follows:

$$\text{MI}(I_{df}; I_{os}) = \mathbb{D}_{\text{KL}}(P(I_{df}, I_{os}) || P(I_{df}) \otimes P(I_{os})),$$

where  $P(\cdot, \cdot)$  is the joint probability distribution,  $P(\cdot)$  denotes the marginal probability distribution, and  $\mathbb{D}_{\text{KL}}$  is the Kullback–Leibler divergence (Joyce 2011).

Since the probability densities  $P(I_{df}, I_{os})$  and  $P(I_{df}) \otimes P(I_{os})$  are unknown, it is difficult to directly minimize  $\text{MI}(I_{df}; I_{os})$ . Inspired by (Belghazi et al. 2018; Hjelm et al. 2019), we construct a mutual information estimation network  $T$  (acting as the discriminator in GANs (Goodfellow et al. 2020)), represented as  $T(\phi; \cdot) : \mathbb{R}^{d_{I_X}} \rightarrow \mathbb{R}$  with parameterizes  $\phi$ , to minimize the  $\text{MI}(I_{df}; I_{os})$  through maximizing its lower-bound Jensen-Shannon divergence (Menéndez et al. 1997), where  $d_{I_X}$  is the dimension of  $I_X$ . While the target of previously designed information decomposition module (acting as the generator in GANs) is to minimize the correlation value between  $I_{df}$  and  $I_{os}$  to achieve a sufficient separation. Specifically, we have the following learning objective:

$$\begin{aligned} \mathcal{L}_{dec} &= \min_{\theta, \psi} \max_{\phi} (\mathbb{E}_{x \sim P(I_{df}, I_{os})} [\log \sigma(T(\phi; x))] \\ &\quad + \mathbb{E}_{x \sim P(I_{df}) \otimes P(I_{os})} [\log (1 - \sigma(T(\phi; x)))]), \end{aligned}$$

where  $\sigma$  is the sigmoid function.

To make the above min-max game be accomplished via standard back-propagation (BP) training, we add a Gradient Reversal Layer (GRL) (Ganin and Lempitsky 2015) before network  $T$  (shown in Fig. 2). In the back-propagation procedure, GRL transmits the gradient by multiplying a negative scalar  $-\beta$  from the subsequent layer to the preceding layer, where we set  $\beta \in (0, 1)$  in practice. This trick is also used in several existing works such as (Belghazi et al. 2018; Hjelm et al. 2019). The network  $T$  consists of three convolution layers (a ReLU activation follows each layer) and a fully connected (FC) layer.

### 3.4 Robust Deepfake Classification Module

After we obtain deepfake-related information  $I_{df}$ , we need to consider how to use it to learn a deepfake detection model. In the literature, the Binary Cross-entropy (BCE) loss is widely used to train a deepfake detection model. However, it is well known that the BCE loss is not robust to imbalance data, especially for deepfake datasets. Using the BCE loss to train models on a certain deepfake dataset may cause significant performance degradation when testing on another deepfake dataset (Pu et al. 2022).

With this observation, we propose a robust deepfake detection loss to enhance the generalization ability of the trained model using deepfake-related information  $I_{df}$  instead of complete information  $I_X$ . Our loss is inspired by the AUC metric since it is a robust measure to evaluate the classification capability of a model, especially when facing imbalanced data. Specifically, it estimates the size of the area under the receiver operating characteristic (ROC) curve (AUC) (He and Garcia 2009), which is composed of False Positive Rates (FPRs) and True Positive Rates (TPRs). However, the AUC metric cannot be directly used as a loss function since it is challenging to compute during each training iteration. Inspired by (Pu et al. 2022), we use the normalized WMW statistic (Yan et al. 2003), equivalent to AUC, to design our loss function.

Specifically, we define a set of indices of fake instances and real instances as  $\mathcal{F} = \{i | Y_i = 1\}$  and  $\mathcal{R} = \{i | Y_i = 0\}$ , respectively. We add a multilayer perceptron (MLP)  $C : \mathbb{R}^{d_{I_X}} \rightarrow \mathbb{R}$  parameterized by  $\omega$  to distinguish fake and real instances, where the input is  $I_{df}$  and the output is a real value. Network  $C$  predicts input  $I_{df}$  to be fake with probability  $\sigma(C(\omega; I_{df}))$ . Without loss of generality,  $C(\omega; I_{df})$  induces the prediction rule such that the predicted label of  $I_{df}$  can be  $\mathbb{I}[\sigma(C(\omega; I_{df})) \geq 0.5]$ , where  $\mathbb{I}[\cdot]$  is an indicator function with  $\mathbb{I}[a] = 1$  if  $a$  is true and 0 otherwise. For simplicity, we assume  $C(\omega; I_{df}^{X_i}) \neq C(\omega; I_{df}^{X_j})$  for any  $X_i \neq X_j$  (ties can be broken in any consistent way), where  $I_{df}^{X_i}$  represents the deepfake information of sample  $X_i$ . We use an alternative version of the normalized WMW defined as follows because WMW is non-differentiable due to its indicator function:

$$\mathcal{L}_{\text{AUC}} = \frac{1}{|\mathcal{F}| |\mathcal{R}|} \sum_{i \in \mathcal{F}} \sum_{j \in \mathcal{R}} E(C(\omega; I_{df}^{X_i}), C(\omega; I_{df}^{X_j})),$$

Methods	Intra-dataset		Cross-dataset	
	AUC $\uparrow$	EER $\downarrow$	AUC $\uparrow$	EER $\downarrow$
Multi-task (Nguyen et al. 2019)	0.763	-	0.543	-
Two Branch (Masi et al. 2020)	0.931	-	0.734	-
MDD (Zhao et al. 2021a)	<b>0.998</b>	-	0.674	-
RL (Nadimpalli and Rattani 2022)	0.994	<b>0.022</b>	0.669	0.362
F <sup>3</sup> -Net (Qian et al. 2020)	0.981	-	0.651	-
CFFs (Yu et al. 2022)	0.976	-	0.742	-
NoiseDF (Wang and Chow 2023)	0.940	-	0.759	-
DID (Ours)	0.970	0.074	<b>0.779</b>	<b>0.286</b>

Table 1: Performance comparison with the baselines in both **intra-dataset** and **cross-dataset** scenarios.

with

$$E(C(\omega; I_{df}^{X_i}), C(\omega; I_{df}^{X_j})) := \begin{cases} -(C(\omega; I_{df}^{X_i}) - C(\omega; I_{df}^{X_j}) - \gamma)^p, & C(\omega; I_{df}^{X_i}) - C(\omega; I_{df}^{X_j}) < \gamma, \\ 0, & \text{otherwise,} \end{cases} \quad (1)$$

where  $|\mathcal{F}|$  and  $|\mathcal{R}|$  are the cardinality of  $\mathcal{F}$  and  $\mathcal{R}$ , respectively;  $0 < \gamma \leq 1$  and  $p > 1$  are two hyperparameters. We combine this AUC loss and the conventional BCE loss  $\mathcal{L}_{\text{BCE}} := -\frac{1}{n} \sum_{i=1}^n [Y_i \cdot \log(\sigma(C(\omega; I_{df}^{X_i}))) + (1 - Y_i) \cdot \log(1 - \sigma(C(\omega; I_{df}^{X_i})))]$  to construct a learning objective for robust deepfake classification:

$$\mathcal{L}_{cls} = \alpha \mathcal{L}_{\text{BCE}} + (1 - \alpha) \mathcal{L}_{\text{AUC}} \quad (2)$$

where  $\alpha$  is a hyperparameter designed to balance the weights of the BCE loss and the AUC loss.

### 3.5 Domain Classification Module

A domain classification module is also designed using another MLP  $\bar{C} : \mathbb{R}^{d_{IX}} \rightarrow \mathbb{R}^{k+1}$  parameterized by  $\bar{\omega}$  for mapping the forgery method related domain information  $I_{dom}$  into a  $(k+1)$ -dimensional domain vector. Specifically, we have  $\bar{C}(\bar{\omega}; I_{dom}) = [\bar{C}^0(\bar{\omega}; I_{dom}), \bar{C}^1(\bar{\omega}; I_{dom}), \dots, \bar{C}^k(\bar{\omega}; I_{dom})]^\top$ , where  $\bar{C}^j(\bar{\omega}; I_{dom})$  is the  $j$ -th domain prediction. We then apply the softmax function to compute the probability of each domain that  $I_{dom}$  belongs to, and combine its domain label to construct a domain classification loss based on the cross-entropy (CE) loss. Therefore, we have

$$\mathcal{L}_{dom} = -\frac{1}{n} \sum_{i=1}^n \sum_{j=0}^k D_i^j \log(S[\bar{C}^j(\bar{\omega}; I_{dom}^{X_i})])$$

where  $S[\bar{C}^j(\bar{\omega}; I_{dom}^{X_i})] \in (0, 1)$  is the  $j$ -th domain predicted probability for the domain information of  $I_{X_i}$  after using softmax operator  $S[\cdot]$ .

**Overall Loss.** To sum up, the proposed framework is optimized with the following final loss function:

$$\mathcal{L} = \lambda_{dec} \mathcal{L}_{dec} + \lambda_{cls} \mathcal{L}_{cls} + \lambda_{dom} \mathcal{L}_{dom} \quad (3)$$

where  $\lambda_{dec}$ ,  $\lambda_{cls}$ , and  $\lambda_{dom}$  are hyperparameters that can balance these loss terms. In the testing phase, only the feature extractor  $G$ , attention module  $A_{df}$ , and the deepfake classification module  $C$  are used.

Models	AUC $\uparrow$	EER $\downarrow$
ResNet50 + BCE	0.620	0.411
<b>ResNet50 + DID</b>	<b>0.727</b>	<b>0.332</b>
EfficientNet-v2-L + BCE	0.716	0.344
<b>EfficientNet-v2-L + DID</b>	<b>0.763</b>	<b>0.302</b>

Table 2: Cross-dataset deepfake detection performance (training on the subset of the DFFD dataset and testing on the Celeb-DF v2 dataset).

## 4 Experiments

This section evaluates the effectiveness of the proposed framework (i.e., DID) in terms of cross-dataset deepfake detection performance. In the following, we will exchange the “method” or “framework” used for DID.

### 4.1 Experimental Settings

**Datasets.** For fair comparisons with the state-of-the-art methods, the two most popular FF++ (Rossler et al. 2019) and Celeb-DF (Li et al. 2020b) datasets are adopted in our experiments. In particular, the high-quality (HQ, with a constant compression rate factor of 23) version of FF++ is used in all of our experiments, which contains one real video subset and four fake video subsets that are generated by using FaceSwap, DeepFakes, Face2Face, and Neural Textures techniques, respectively. Each subset contains 1000 videos, in which 720/140/140 videos are used for training/validation/test, respectively. The Celeb-DF dataset contains real and fake videos according to 59 celebrities. Following the official protocols in (Li et al. 2020b), we use the latest version of Celeb-DF named Celeb-DF V2, which contains 590 real celebrity (Celeb-real) videos, 300 real videos downloaded from YouTube (YouTube-real), and 5639 synthesized celebrity (Celeb-synthesis) videos based on Celeb-real.

#### Compared Methods and Evaluation Metrics.

To evaluate the effectiveness of our framework, we compare it with the following state-of-the-art (SOTA) frame-level baseline methods: F<sup>3</sup>-Net (Qian et al. 2020), CFFs (Yu et al. 2022), RL (Nadimpalli and Rattani 2022), Multi-task (Nguyen et al. 2019), Two Branch (Masi et al. 2020), MDD (Zhao et al. 2021a), and NoiseDF (Wang and Chow 2023). The results of Multi-task and Two Branch are cited from (Nadimpalli and Rattani 2022), and the results of MDD are cited from (Yu et al. 2022). We consider two evaluation metrics, the area under the receiver operating characteristic curve (AUC) and the equal error rate (EER), which are widely adopted in previous works.

**Implementation Details.** In our experiments, EfficientNet v2-L (Tan and Le 2021) pre-trained on the ImageNet dataset is adopted as the backbone for feature extraction. Face images in all frames are aligned to  $224 \times 224$  using the MTCNN (Zhang et al. 2016) method. Then they are converted into the grayscale from the RGB before sending to the proposed framework. The framework is trained with the Adam optimizer with a weight decay of  $5e^{-4}$  and a learning rate of  $1e^{-5}$ . The batch size is 15 and the number of iterations in each epoch is 6000. We set  $\gamma$  and  $p$  in Eq. (1) to 0.15 and

Models	Modules			AUC $\uparrow$	EER $\downarrow$
	$A_{df}$	$A_{dom}$	$T$		
w/o $A_{dom}$	$\checkmark$	$\times$	$\checkmark$	0.763	0.302
w/o $T$	$\checkmark$	$\checkmark$	$\times$	0.759	0.305
DID	$\checkmark$	$\checkmark$	$\checkmark$	0.779	0.286

Table 3: Ablation study by removing the domain attention module  $A_{dom}$  (“w/o  $A_{dom}$ ”) or the decorrelation learning module  $T$  (“w/o  $T$ ”) from the DID framework.

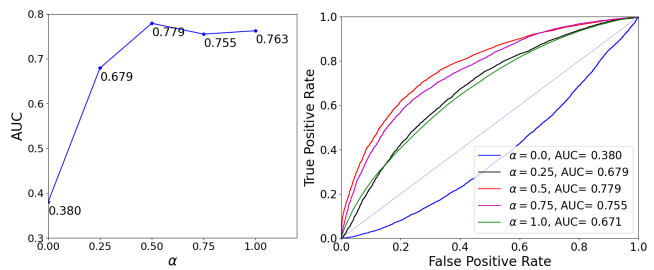
2, respectively. We use  $\alpha = 0.5$  in Eq. (2). Hyperparameters  $\lambda_{cls}$ ,  $\lambda_{dom}$ , and  $\lambda_{dec}$  in Eq. (3) are set to 1.0, 1.0, and 0.01, respectively. Hyperparameter  $\beta$  increases from 0 to 1 in the training procedure as  $\beta = 2.0 / (1.0 + e^{-5p}) - 1.0$ , where  $p$  is the ratio of current training epochs to the maximum training epochs. All experiments are performed on two NVIDIA RTX 3080 GPUs, with Pytorch 1.10 and Python 3.6.

## 4.2 Experimental Results

**Intra-dataset Evaluation.** We evaluate the detection performance of our proposed method DID in the intra-dataset situation, where the training and test sets are from the FF++ dataset and disjoint. Tab. 1 shows the intra-dataset evaluation results and comparison with the baselines. Our method outperforms Multi-task (Nguyen et al. 2019) and Two Branch (Masi et al. 2020) methods, and is competitive with the best performance (0.998 on AUC score achieved by MDD (Zhao et al. 2021a), and 0.022 on EER achieved by RL (Nadimpalli and Rattani 2022)).

**Cross-dataset Evaluation.** The cross-dataset generalization performance of the proposed method and comparison with the baselines are also shown in Tab. 1. All models are first trained on the training set of the FF++ dataset and then tested on the test set of Celeb-DF v2 (unseen during training). From the table, it is evident that the performance of all methods significantly degrades in the cross-dataset scenario when compared to the intra-dataset scenario. However, in this cross-dataset scenario, DID exceeds the best performer of the baselines, CFFs (Yu et al. 2022), by a margin of 4.99% (0.779 vs. 0.742) on AUC, and reduces EER to 0.286 from RL’s 0.362 (the best performance of the baselines), with a performance improvement of 20.99%. These experimental results validate the effectiveness and superiority of our framework.

**Effect on Different Training Dataset.** To further demonstrate the applicability of our methods, we train the DID framework on the DFFD dataset (Dang et al. 2020) and evaluate the detection performance on the Celeb-DF dataset. DFFD is a deepfake dataset composing real images, the corresponding deepfake images created with FaceSwap (Faceswap), Deepfakes (Deepfakes), Face2Face (Thies et al. 2016), FaceAPP (Faceapp), StarGAN (Choi et al. 2018), PGGAN (Karras et al. 2018) (two versions), and StyleGAN (Karras, Laine, and Aila 2019a) methods, and deepfake videos generated by Deep Face Lab (DeepFaceLab). The experiments are conducted on a subset of DFFD (except for the deepfake videos, which are unable to access) following the protocols of (Dang et al. 2020), with different



(a) AUC with different  $\alpha$

(b) ROC with different  $\alpha$

Figure 3: Effect of different  $\alpha$  values (used as the balance factor between BCE and AUC loss) on the AUC score.

feature extraction backbones. Tab. 2 shows the experimental results. We can see that DID achieves great performance improvement on all backbones fine-tuned with the BCE loss. Specifically, the improvement relative to the ResNet50 backbone (fine-tuned with the BCE loss) is 17.26% on AUC and 19.22% on EER. Meanwhile, the improvement relative to the EfficientNet-v2-L backbone is 6.56% on AUC and 12.21% on EER. These results demonstrate the applicability of our methods on other datasets and different feature extraction backbones in cross-dataset deepfake detection.

## 4.3 Ablation Study

**The Effect of AUC Loss.** The impact of hyperparameter  $\alpha$  in the AUC loss, i.e., Eq. (2), is investigated. Specifically, we train our model with different  $\alpha \in \{0.0, 0.25, 0.5, 0.75, 1.0\}$  values and show the AUC performance in Fig. 3. The model trained with only the AUC loss ( $\alpha=0.0$ ) as the deepfake classification loss function gets the lowest AUC of 0.380, and the model trained with only the BCE deepfake classification loss ( $\alpha=1.0$ ) obtains an AUC of 0.763. However, the model trained with an equal weight of the AUC loss and the BCE loss ( $\alpha=0.5$ ) shows the best AUC score of 0.779, which means the AUC loss can help improve the generalization ability of the model.

**The Effect of  $A_{dom}$  and  $T$  Modules.** To explore the necessity of the domain attention module  $A_{dom}$  and the decorrelation learning module  $T$ , we train the proposed DID framework with either one of the two modules removed. The detection results of these models are shown in Tab. 3. We can see from the table that when the domain attention module  $A_{dom}$  is removed from DID (“w/o  $A_{dom}$ ” in Tab. 3), the AUC score declines by 2.05% (from 0.779 to 0.763) and EER increases by 5.59% (from 0.286 to 0.302) relative to the complete DID version. In addition, the model without the decorrelation learning module  $T$  (“w/o  $T$ ” in Tab. 3) achieves 0.759 on AUC and 0.305 on EER, the performance degradation (relative to DID) is larger than the model w/o  $A_{dom}$ . Specifically, the AUC score drops by 2.57%, and EER increases by 6.64%. These results suggest the indispensability of the DID framework’s  $A_{dom}$  and  $T$  modules.

**Analysis of Domain Classification Module.** Fig. 4 displays the confusion matrix of the domain feature classification. We can see that the domain classification module distinguishes all forgery methods with very high accuracy. Specifically,

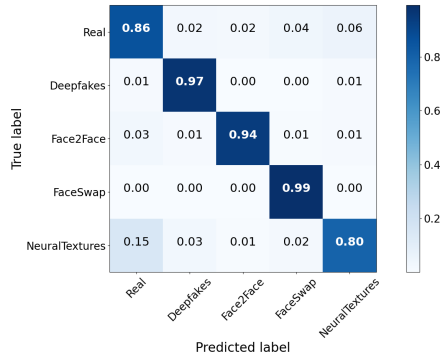


Figure 4: Confusion matrix visualization of domain feature classification.

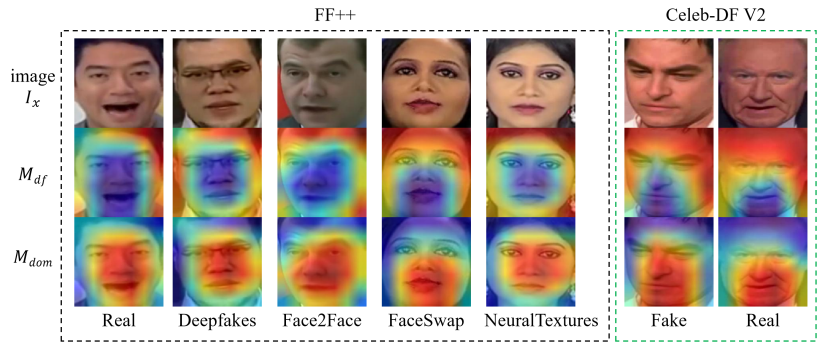


Figure 5: Visualization of the real/fake attention map  $M_{df}$  and the domain attention map  $M_{dom}$  on the FF++ and Celeb-DF v2 datasets.

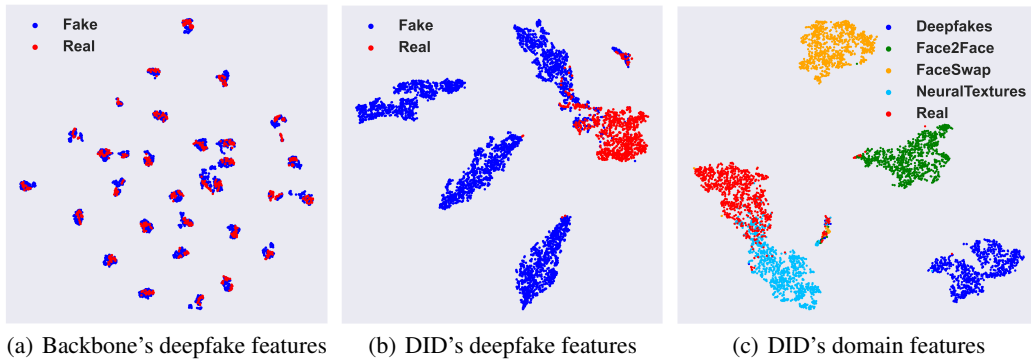


Figure 6: Visualization of deepfake features of the EfficientNet-v2-L backbone network (left) and our DID framework's deepfake features (middle) and domain features (right).

the average accuracy is 0.91, and the highest accuracy is 0.99 (classification of the FaceSwap method). These results indicate that domain information is successfully captured by the domain classification module, which aligns with our decomposition objective.

#### 4.4 Visualization

**Visualization of The Saliency Map.** To more intuitively demonstrate the effectiveness of our method, we visualize the Grad-CAM of deepfake attention  $M_{df}$  and domain (forgery technique) attention  $M_{dom}$  in Fig. 5. We can see that the activation region of  $M_{df}$  and  $M_{dom}$  are different.  $M_{dom}$  focuses on areas such as the nose, mouth, and eyes. In contrast,  $M_{df}$  focuses on the information invariant to forgery techniques. The visualization results demonstrate the effectiveness of our method: the decorrelation learning module promotes the disentangled components to contain different information and be irrelevant to each other.

**Visualization of Deepfake and Domain Features.** Fig. 6(a) and Fig. 6(b) depict the T-SNE visualization of the deepfake feature vectors learned by the backbone network EfficientNet-v2-L and our DID framework, respectively. The red and blue dots in the two figures represent the deepfake features of real and fake facial images, respectively. As illustrated in the figures, the real and fake features learned by

the backbone network are mixed in the space, whereas those learned by our DID framework are well separated in the feature space. This observation suggests the high real/fake discrimination performance of DID's deepfake features.

Fig. 6(c) further presents a visualization of domain features learned by our DID framework. We can see from the figure that the domain features learned from facial images created with different forgery techniques are well separated in the embedding space, with domain features from the same forgery technique being clustered together while those from other forgery techniques are far apart. These results demonstrate that the deepfake technique-related information is well captured and separated in our DID framework.

## 5 Conclusion

We propose a deep information decomposition (DID) framework in this paper. It decomposes the facial information into deepfake-related and unrelated information and optimizes these two kinds of information to be sufficiently separated. Only deepfake-related information is used for real/fake discrimination, which makes the detection model robust to irrelevant changes and generalizable to unseen forgery methods. Extensive experiments and visualizations demonstrate the effectiveness and superiority of the DID framework on cross-dataset deepfake detection tasks.

One limitation of our proposed DID framework is that all hyperparameters included in the loss function need to be manually selected through experiments. In future work, we will optimize these hyperparameters automatically and improve the current domain classification module without using the domain information of the dataset.

## References

- Bao, J.; Chen, D.; Wen, F.; Li, H.; and Hua, G. 2018. Towards open-set identity preserving face synthesis. In *Proceedings of the IEEE Conference on Computer Vision and Pattern Recognition*, 6713–6722.
- Belghazi, M. I.; Baratin, A.; Rajeshwar, S.; Ozair, S.; Bengio, Y.; Courville, A.; and Hjelm, D. 2018. Mutual information neural estimation. In *Proceedings of the International Conference on Machine Learning*, 531–540.
- Choi, Y.; Choi, M.; Kim, M.; Ha, J.-W.; Kim, S.; and Choo, J. 2018. Stargan: Unified generative adversarial networks for multi-domain image-to-image translation. In *Proceedings of the IEEE Conference on Computer Vision and Pattern Recognition*, 8789–8797.
- Dang, H.; Liu, F.; Stehouwer, J.; Liu, X.; and Jain, A. K. 2020. On the detection of digital face manipulation. In *Proceedings of the IEEE Conference on Computer Vision and Pattern Recognition*, 5781–5790.
- DeepFaceLab. Accessed: 2022.10.15. <https://github.com/iperov/DeepFaceLab>.
- Deepfakes. Accessed: 2022.10.15. <https://github.com/iperov/DeepFaceLab>.
- Dong, S.; Wang, J.; Liang, J.; Fan, H.; and Ji, R. 2022a. Explaining deepfake detection by analysing image matching. In *European Conference on Computer Vision*, 18–35.
- Dong, X.; Bao, J.; Chen, D.; Zhang, T.; Zhang, W.; Yu, N.; Chen, D.; Wen, F.; and Guo, B. 2022b. Protecting Celebrities from DeepFake with Identity Consistency Transformer. In *Proceedings of the IEEE Conference on Computer Vision and Pattern Recognition*, 9468–9478.
- Faceapp. Accessed: 2022.10.15. <https://faceapp.com/app>.
- Faceswap. Accessed: 2022.10.15. <https://www.github.com/deepfakes/faceswap>.
- Frank, J.; Eisenhofer, T.; Schönherr, L.; Fischer, A.; Kolossa, D.; and Holz, T. 2020. Leveraging frequency analysis for deep fake image recognition. In *Proceedings of the International Conference on Machine Learning*, 3247–3258.
- Ganin, Y.; and Lempitsky, V. 2015. Unsupervised domain adaptation by backpropagation. In *Proceedings of the International Conference on Machine Learning*, 1180–1189.
- Geng, Z.; Cao, C.; and Tulyakov, S. 2019. 3d guided fine-grained face manipulation. In *Proceedings of the IEEE Conference on Computer Vision and Pattern Recognition*, 9821–9830.
- Goodfellow, I.; Pouget-Abadie, J.; Mirza, M.; Xu, B.; Warde-Farley, D.; Ozair, S.; Courville, A.; and Bengio, Y. 2020. Generative adversarial networks. *Communications of the ACM*, 63(11): 139–144.
- He, H.; and Garcia, E. A. 2009. Learning from imbalanced data. *IEEE Transactions on Knowledge and Data Engineering*, 21(9): 1263–1284.
- He, K.; Zhang, X.; Ren, S.; and Sun, J. 2016. Deep residual learning for image recognition. In *Proceedings of the IEEE Conference on Computer Vision and Pattern Recognition*, 770–778.
- He, R.; Wu, X.; Sun, Z.; and Tan, T. 2017. Learning invariant deep representation for nir-vis face recognition. In *Proceedings of the AAAI Conference on Artificial Intelligence*, volume 31.
- He, R.; Wu, X.; Sun, Z.; and Tan, T. 2018. Wasserstein CNN: Learning invariant features for NIR-VIS face recognition. *IEEE Transactions on Pattern Analysis and Machine Intelligence*, 41(7): 1761–1773.
- Hjelm, R. D.; Fedorov, A.; Lavoie-Marchildon, S.; Grewal, K.; Bachman, P.; Trischler, A.; and Bengio, Y. 2019. Learning deep representations by mutual information estimation and maximization. In *International Conference on Learning Representations*.
- Hu, J.; Wang, S.; and Li, X. 2021. Improving the Generalization Ability of Deepfake Detection via Disentangled Representation Learning. In *IEEE International Conference on Image Processing*, 3577–3581.
- Joyce, J. M. 2011. Kullback-leibler divergence. In *International Encyclopedia of Statistical Science*, 720–722.
- Karras, T.; Aila, T.; Laine, S.; and Lehtinen, J. 2018. Progressive Growing of GANs for Improved Quality, Stability, and Variation. In *International Conference on Learning Representations*.
- Karras, T.; Laine, S.; and Aila, T. 2019a. A style-based generator architecture for generative adversarial networks. In *Proceedings of the IEEE Conference on Computer Vision and Pattern Recognition*, 4401–4410.
- Karras, T.; Laine, S.; and Aila, T. 2019b. A style-based generator architecture for generative adversarial networks. In *Proceedings of the IEEE Conference on Computer Vision and Pattern Recognition*, 4401–4410.
- Kim, D.-K.; and Kim, K.-S. 2022. Generalized Facial Manipulation Detection with Edge Region Feature Extraction. In *Proceedings of the IEEE Winter Conference on Applications of Computer Vision*, 2828–2838.
- Kinney, J. B.; and Atwal, G. S. 2014. Equitability, mutual information, and the maximal information coefficient. *Proceedings of the National Academy of Sciences*, 111(9): 3354–3359.
- Li, J.; Xie, H.; Li, J.; Wang, Z.; and Zhang, Y. 2021. Frequency-aware discriminative feature learning supervised by single-center loss for face forgery detection. In *Proceedings of the IEEE Conference on Computer Vision and Pattern Recognition*, 6458–6467.
- Li, L.; Bao, J.; Zhang, T.; Yang, H.; Chen, D.; Wen, F.; and Guo, B. 2020a. Face x-ray for more general face forgery detection. In *Proceedings of the IEEE Conference on Computer Vision and Pattern Recognition*, 5001–5010.

- Li, Y.; Chang, M.-C.; and Lyu, S. 2018. In icu oculi: Exposing ai created fake videos by detecting eye blinking. In *IEEE International Workshop on Information Forensics and Security*, 1–7.
- Li, Y.; and Lyu, S. 2019. Exposing deepfake videos by detecting face warping artifacts. *Proceedings of the IEEE Conference on Computer Vision and Pattern Recognition Workshops*.
- Li, Y.; Yang, X.; Sun, P.; Qi, H.; and Lyu, S. 2020b. Celebdf: A large-scale challenging dataset for deepfake forensics. In *Proceedings of the IEEE Conference on Computer Vision and Pattern Recognition*, 3207–3216.
- Liang, J.; Shi, H.; and Deng, W. 2022. Exploring Disentangled Content Information for Face Forgery Detection. In *Proceedings of the European Conference on Computer Vision*, 128–145.
- Luo, Y.; Zhang, Y.; Yan, J.; and Liu, W. 2021. Generalizing face forgery detection with high-frequency features. In *Proceedings of the IEEE Conference on Computer Vision and Pattern Recognition*, 16317–16326.
- Masi, I.; Killekar, A.; Mascarenhas, R. M.; Gurudatt, S. P.; and AbdAlmageed, W. 2020. Two-branch recurrent network for isolating deepfakes in videos. In *Proceedings of the European Conference on Computer Vision*, 667–684.
- Menéndez, M.; Pardo, J.; Pardo, L.; and Pardo, M. 1997. The jensen-shannon divergence. *Journal of the Franklin Institute*, 334(2): 307–318.
- Nadimpalli, A. V.; and Rattani, A. 2022. On improving cross-dataset generalization of deepfake detectors. In *Proceedings of the IEEE Conference on Computer Vision and Pattern Recognition*, 91–99.
- Neves, J. C.; Tolosana, R.; Vera-Rodriguez, R.; Lopes, V.; Proença, H.; and Fierrez, J. 2020. Ganprintr: Improved fakes and evaluation of the state of the art in face manipulation detection. *IEEE Journal of Selected Topics in Signal Processing*, 14(5): 1038–1048.
- Nguyen, H. H.; Fang, F.; Yamagishi, J.; and Echizen, I. 2019. Multi-task learning for detecting and segmenting manipulated facial images and videos. In *IEEE International Conference on Biometrics Theory, Applications and Systems*, 1–8. IEEE.
- Nguyen, T. T.; Nguyen, Q. V. H.; Nguyen, D. T.; Nguyen, D. T.; Huynh-The, T.; Nahavandi, S.; Nguyen, T. T.; Pham, Q.-V.; and Nguyen, C. M. 2022. Deep learning for deepfakes creation and detection: A survey. *Computer Vision and Image Understanding*, 223: 103525.
- Pu, W.; Hu, J.; Wang, X.; Li, Y.; Hu, S.; Zhu, B.; Song, R.; Song, Q.; Wu, X.; and Lyu, S. 2022. Learning a deep dual-level network for robust DeepFake detection. *Pattern Recognition*, 130: 108832.
- Pumarola, A.; Agudo, A.; Martinez, A.; Sanfeliu, A.; and Moreno-Noguer, F. 2018. GANimation: Anatomically-aware Facial Animation from a Single Image. In *Proceedings of the European Conference on Computer Vision*.
- Qian, Y.; Yin, G.; Sheng, L.; Chen, Z.; and Shao, J. 2020. Thinking in frequency: Face forgery detection by mining frequency-aware clues. In *Proceedings of the European Conference on Computer Vision*, 86–103.
- Rössler, A.; Cozzolino, D.; Verdoliva, L.; Riess, C.; Thies, J.; and Nießner, M. 2019. Faceforensics++: Learning to detect manipulated facial images. In *Proceedings of the IEEE International Conference on Computer Vision*, 1–11.
- Shiohara, K.; and Yamasaki, T. 2022. Detecting Deepfakes with Self-Blended Images. In *Proceedings of the IEEE Conference on Computer Vision and Pattern Recognition*, 18720–18729.
- Tan, M.; and Le, Q. 2021. Efficientnetv2: Smaller models and faster training. In *Proceedings of the International Conference on Machine Learning*, 10096–10106.
- Thies, J.; Zollhöfer, M.; and Nießner, M. 2019. Deferred neural rendering: Image synthesis using neural textures. *ACM Transactions on Graphics (TOG)*, 38(4): 1–12.
- Thies, J.; Zollhofer, M.; Stamminger, M.; Theobalt, C.; and Nießner, M. 2016. Face2face: Real-time face capture and reenactment of rgb videos. In *Proceedings of the IEEE Conference on Computer Vision and Pattern Recognition*, 2387–2395.
- Tran, L.; Yin, X.; and Liu, X. 2017. Disentangled representation learning gan for pose-invariant face recognition. In *Proceedings of the IEEE Conference on Computer Vision and Pattern Recognition*, 1415–1424.
- Wang, H.; Gong, D.; Li, Z.; and Liu, W. 2019. Decorrelated adversarial learning for age-invariant face recognition. In *Proceedings of the IEEE Conference on Computer Vision and Pattern Recognition*, 3527–3536.
- Wang, T.; and Chow, K. P. 2023. Noise Based Deepfake Detection via Multi-Head Relative-Interaction. In *Proceedings of the AAAI Conference on Artificial Intelligence*, volume 37, 14548–14556.
- Wu, X.; Huang, H.; Patel, V. M.; He, R.; and Sun, Z. 2019. Disentangled variational representation for heterogeneous face recognition. In *Proceedings of the AAAI Conference on Artificial Intelligence*, volume 33, 9005–9012.
- Yan, L.; Dodier, R. H.; Mozer, M.; and Wolniewicz, R. H. 2003. Optimizing classifier performance via an approximation to the Wilcoxon-Mann-Whitney statistic. In *Proceedings of the International Conference on Machine Learning*, 848–855.
- Yang, S.; Yang, X.; Lin, Y.; Cheng, P.; Zhang, Y.; and Zhang, J. 2021. Heterogeneous Face Recognition with Attention-guided Feature Disentangling. In *Proceedings of the 29th ACM International Conference on Multimedia*, 4137–4145.
- Yang, X.; Li, Y.; and Lyu, S. 2019. Exposing deep fakes using inconsistent head poses. In *IEEE International Conference on Acoustics, Speech and Signal Processing*, 8261–8265.
- Yu, P.; Fei, J.; Xia, Z.; Zhou, Z.; and Weng, J. 2022. Improving Generalization by Commonality Learning in Face Forgery Detection. *IEEE Transactions on Information Forensics and Security*, 17: 547–558.

Zhang, K.; Zhang, Z.; Li, Z.; and Qiao, Y. 2016. Joint face detection and alignment using multitask cascaded convolutional networks. *IEEE Signal Processing Letters*, 23(10): 1499–1503.

Zhang, T. 2022. Deepfake generation and detection, a survey. *Multimedia Tools and Applications*, 81(5): 6259–6276.

Zhao, H.; Zhou, W.; Chen, D.; Wei, T.; Zhang, W.; and Yu, N. 2021a. Multi-attentional deepfake detection. In *Proceedings of the IEEE Conference on Computer Vision and Pattern Recognition*, 2185–2194.

Zhao, T.; Xu, X.; Xu, M.; Ding, H.; Xiong, Y.; and Xia, W. 2021b. Learning self-consistency for deepfake detection. In *Proceedings of the IEEE/CVF International Conference on Computer Vision*, 15023–15033.